EFFECT OF THE FIRST AXIAL FIELD SPECTROMETER IN THE CERN INTERSECTING STORAGE RINGS (ISR) ON THE CIRCULATING BEAMS

P.J.Bryant and G.Kantardjian

CERN, Geneva, Switzerland

Introduction and General Description

In 1973, the CERN-Columbia-Rockefeller Collaboration proposed the use of a solenoid spectrometer[1] in the ISR. This spectrometer, shown in Fig. 1, consists of a superconducting solenoid magnet[2], cylindrical drift chambers, scintillation counters and two arrays of lead glass Cerenkov counters. The axis of the solenoid is on the bisector of the two undisturbed beam paths at intersection 1 in the ISR. The layout can be seen in Figs. 1 and 2. The coil is surrounded by an iron flux return path. The two end plates have slots for the passage of the vacuum chambers. The effect on a circulating beam of such a device was first investigated using a small test solenoid. Table 1 summarizes the main features of the superconducting solenoid and the conventional test solenoid.

TABLE 1

		Test solenoid	Superconducting solenoid
Nominal central field	(T)	1.5	1.5
Integrated axial field	(Tm)	0.5	2.7
Length of the inner volume	(mm)	300	1800
Overall length	(mm)	460	3120
Inner diameter	(mm)	260	1380
Vertical aperture in end piece	(mm)	80	200
Horizontal aperture in end piece	(mm)	256	1350

As the solenoid axis is set at an angle of 7.4° with respect to both beams, the radial component of the field gives a vertical kick which is compensated by two dipole magnets upstream and downstream of the solenoid in each beam. Table 2 gives the main features of these radial field compensators[3].

TABLE 2

Nominal field	0.53	T
Steel length	500	mm
Overall length	779	mm
Gap height	210	mm

The ISR low-β insertion[4], which was originally installed in intersection 7, was moved to intersection 1 for operation with the solenoid. To facilitate access

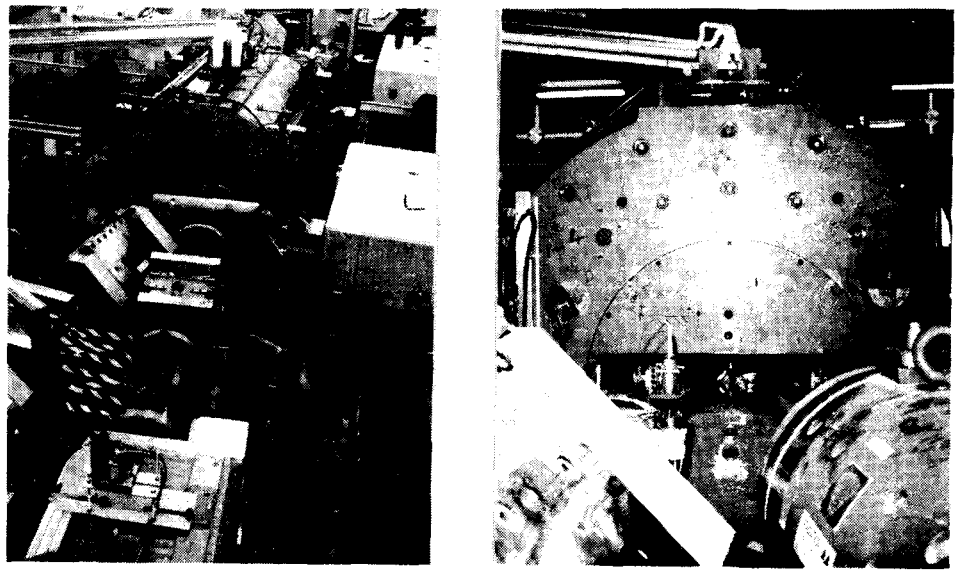

Fig. 1 Solenoid in Intersection I1 and End View Showing Horizontal Slots in End Plates

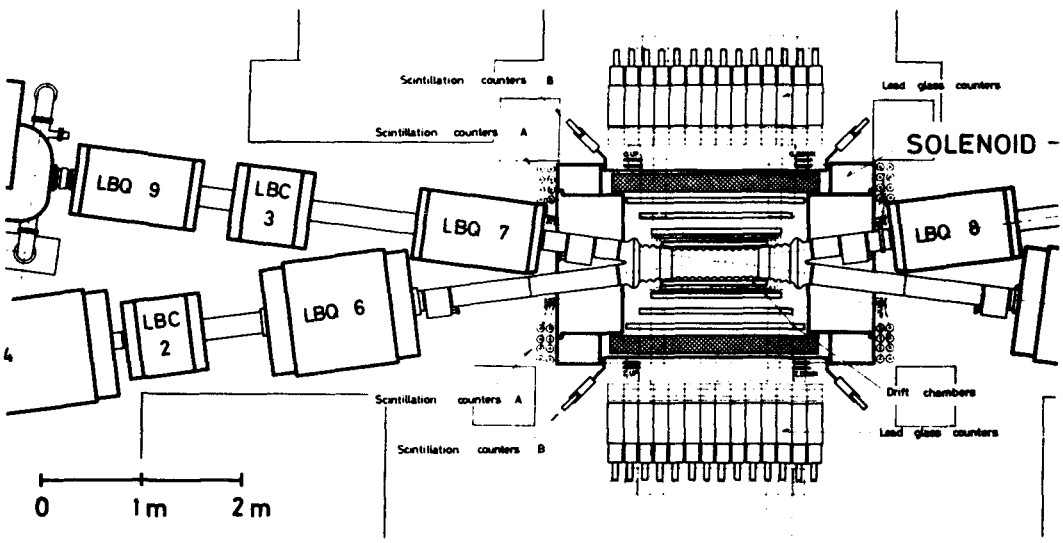

Fig. 2 Layout in Intersection I1

to the solenoid, the innermost quadrupoles were mounted on rails and the dipole compensators were made demountable. The low-β insertion increases the luminosity by a factor of 2.3.

Bending and Focusing Effects

The effect on the closed orbit arises from a gyration of the beam in the central axial field and from horizontal deflections in the end plates. The gyration

appears principally as a vertical kick of 4 mrad (full field and 26 GeV/c) which is corrected by nearby dipole magnets on each side of the solenoid. The resultant orbit bump lifts the interaction diamond by 8.8 mm. A small asymmetry in the position of the dipole compensators causes a residual horizontal kick of 8 μrad. The beam traverses the end-plate slots at 6 - 7 mm above the median plane and, as a result, the vertical skew fields kick the beam horizontally. Fortunately, the end fields are partially compensating and only 1 mm peak-to-peak is added to the horizontal closed orbit. Rather than trying to correct this distortion locally in an already crowded intersection, it is allowed to propagate into the ISR lattice where it is corrected by the normal orbit correction elements. In order to take the detailed structure of the field into account, the beam trajectories were first determined using a field plot.

The form of the solenoid's end field is an important factor in the design. End plates with horizontal slots, rather than open ends or end plates with circular holes, were chosen for a variety of reasons. The internal axial field is more uniform, the vertical dispersion is eliminated and for the configuration of beam parameters in the ISR the coupling is minimized.

The focusing strength of such a solenoid is very weak and the theoretical tune shift of 0.0005 could not be detected.

Excitation of the $Q_x - Q_z = 0$ Resonances

The ISR are normally operated with the horizontal and vertical tunes separated by 0.01 or 0.02 in order to take advantage of the large, resonance-free regions close to the diagonal in the tune diagram. To prevent luminosity loss due to coupling blowing up the vertical beam size, the linear coupling resonance $Q_x - Q_z = 0$ is strictly controlled. Coupling can also perturb tune measurements and some injection optimization systems. Stacks crossing this resonance often have a higher decay rate. The coupling coefficient C or driving term for this resonance is[5]

$$C = \frac{1}{2\pi R}\int_0^{2\pi}\sqrt{\beta_x\beta_z}\left[K + \frac{1}{2}MR\left(\frac{\alpha_x}{\beta_x} - \frac{\alpha_z}{\beta_z}\right) - \frac{i}{2}MR\left(\frac{1}{\beta_x} + \frac{1}{\beta_z}\right)\right]$$
$$\exp\left[i\left\{\int_0^{\theta}\left(\frac{R}{\beta_x(\phi)} - Q_x\right)d\phi - \int_0^{\theta}\left(\frac{R}{\beta_z(\phi)} - Q_z\right)d\phi + \theta\right\}\right]d\theta ,$$

where:

β_x, β_z = horizontal and vertical betatron amplitudes,

$\theta = s/R$ where s = azimuthal distance along beam, R = average machine radius,

$\alpha_{x,z} = -\frac{1}{2}\,d\beta_{x,z}/ds$; $K(\theta) = \frac{1}{2}\frac{R^2}{|B\rho|}\left(\frac{\partial B_x}{\partial x} - \frac{\partial B_z}{\partial z}\right)$; $M(\theta) = \frac{R}{|B\rho|}B_s$,

B_x, B_z, B_s = horizontal, vertical and axial field components, respectively,

$|B\rho|$ = magnetic rigidity.

Thus, C is an integral around the whole machine over all skew gradients and axial fields. Its phase in the complex plane depends on the origin in θ, i.e. the observation point, but its magnitude is independent of this origin. Once C is known, either by calculation or measurement[6], all effects[5,7] arising from coupling can be calculated.

Solenoids and End-Plate Design

The axial field in a solenoid will contribute to C via two terms in the above formula.

Principal Axial Field Term:

$$-\frac{i}{4\pi}\sqrt{\beta_x\beta_z}\,\frac{RB_s}{|B\rho|}\left(\frac{1}{\beta_x}+\frac{1}{\beta_z}\right) \quad \text{(phase term)}$$

Second Axial Field Term:

$$\frac{1}{4\pi}\sqrt{\beta_x\beta_z}\,\frac{RB_s}{|B\rho|}\left(\frac{\alpha_x}{\beta_x}-\frac{\alpha_z}{\beta_z}\right) \quad \text{(phase term)} \ .$$

The principal term has an imaginary amplitude which increases as the β-values decrease. When the ISR solenoid is run with the low-β insertion[4], the coupling from this term is twice that arising in normal operation. The second term is, in general, small and has a real amplitude.

The end fields of the solenoid contribute to C via one term, namely:

End-Plate or Skew Quadrupole Term:

$$\frac{1}{4\pi}\sqrt{\beta_x\beta_z}\,\frac{R}{|B\rho|}\left(\frac{\partial B_x}{\partial x}-\frac{\partial B_z}{\partial z}\right) \quad \text{(phase term)} \ .$$

It is clear that if the solenoid is open or has a circular aperture in its end plate, this term is zero, but if there is a slot, the contribution can be large and will have a real amplitude.

The action of the phase term can be very important. In the case of the ISR low-β insertion[4], the vertical betatron phase advances far more rapidly than the horizontal phase and, as a result, the phase term from the formula in the preceding chapter acts so as to rotate and combine the two end-plate vectors such that their resultant compensates the axial field terms. Without the low-β insertion, the vertical phase advance is still larger than the horizontal one but the difference is smaller and the mutual compensation between axial and end fields is less effective. Table 3 illustrates the axial field and end-plate field compensation effect using calculated values, and also gives the measured values for the overall coupling.

The ELSA working line and the low-β insertion mentioned in Table 3 are the most frequently used operating conditions. In both cases, $\Delta = Q_x - Q_z = 0.02$ (i.e.

TABLE 4

Measured and Calculated Values for the Coupling Excitation Due to the ISR Solenoid (Full Field, 26 GeV/c)

	Calculated			Measured*
	Re(C)	Im(C)	|C|	|C|
ELSA Working Line:				
Principal axial field term	0.00076	-0.00496	0.00502	--
Second axial field term	0.00068	0.00010	0.00069	--
End plates	-0.00027	0.00175	0.00177	--
Totals	0.00118	-0.00311	0.00333	0.0036
Low-β insertion:				
Principal axial field term	0.00297	-0.01010	0.01052	--
Second axial field term	-0.00078	0.00060	0.00098	--
End plates	-0.00280	0.01272	0.01303	--
Totals	-0.00061	0.00202	0.00211	0.0024

* At present, only $|C|$ can be measured directly in the ISR.

the working line is parallel to the $Q_x - Q_z = 0$ resonance). The compensation between the end plates and central field makes $|C|$ less than $|\Delta|/5$ and no further compensation is needed. The theoretical luminosity losses are small (Table 5), but there is still an interest in keeping a strict control on the working line, since if, for example, Δ drops to 0.01 the luminosity loss on ELSA becomes -7.6 % for unshaved beams and -9.8 % for 50 % shaving.

TABLE 5

Calculated Luminosity Losses Due to Coupling

Working condition:	ELSA	Low-β
$\Delta \approx Q_x - Q_z$	0.02	0.02
Coupling, $\|C\|$	3.6×10^{-3}	2.4×10^{-3}
Initial emittance ratio	2.0	2.0
Luminosity losses:		
No shaving	-2.2 %	-1.0 %
50 % shaving	-3.5 %	-1.6 %

It would be possible to arrange the low-β insertion in such a way that the phase advances and β-functions would give a perfect compensation between end plates and central field. It should be noted that in the coupling matrix for the whole machine, the coupling coefficients would not be zero in this case. The effect of

making C = 0 is to re-arrange the matrix so that the $Q_x - Q_z = 0$ resonance is not excited. However, some other resonances will always be excited, but for the ISR, only $Q_x - Q_z = 0$ is of importance.

High Order Nonlinear Resonances

A mainly qualitative idea of nonlinear resonance excitation was obtained by accelerating a beam across the machine aperture and recording the current losses when resonances were crossed. There was no excitation of resonances above the 5th order, and for 5th order resonances the excitation was comparable to the beam-beam excitation. Since resonances below 8th order are not tolerated inside stacks, the solenoid does not detectably add to the loss rate.

ISR Performance with the Solenoid

After only 14 hours of machine development, the solenoid became operational for physics in December 1976 and by early May 1977 it had been used for 800 hours of colliding beam physics at 26 and 31 GeV/c. No operational restrictions have been imposed on the ISR by the solenoid and physics conditions have not been in any way degraded. In the most recent low-β run at 26 GeV/c with the solenoid, the beam currents were 27×27 A^2 and the starting luminosity was 3.6×10^{31} cm^{-2}s^{-1} with an average beam decay rate of 3×10^{-6} min^{-1} over the 63-hour run.

For the eventuality of a cryogenic failure, a computer program has been successfully tested[8] for switching off the solenoid and its compensators without disturbing the circulating beams. The beams are stacked with the solenoid at full power.

Acknowledgements

The authors would especially like to thank M. Morpurgo and S. Pichler for their help and all the people whose work made the operation of the solenoid successful.

References

1. Experimental Proposal ISRC 73-13 (1973).
2. M. Morpurgo, Design and construction of a superconducting aluminium stabilized solenoid, Cryogenics Vol. 17, No. 2 (1977).
3. S. Pichler, F. Schäff, A. Verdier, Private communication.
4. J.P. Gourber, E. Keil, S. Pichler, Div. Report CERN ISR-MA/75-8 (1975).
5. G. Guignard, CERN Report 76-06 (1976).
6. P.J. Bryant et al., Div. Report CERN ISR-BOM/77-4 (1977).
7. G. Guignard, Beam blow-up and luminosity reduction due to linear coupling, Report to be published.
8. K. Brand, J. Gamble, D. Lewis, Private communication.